A HIGH SENSITIVITY SOI ELECTRIC-FIELD SENSOR WITH NOVEL COMB-SHAPED MICROELECTRODES

Pengfei Yang[1, 2], Chunrong Peng[1], Haiyan Zhang[1, 2], Shiguo Liu[1], Dongming Fang[1], and Shanhong Xia[1,]*
[1]State Key Laboratory of Transducer Technology, Institute of Electronics, Chinese Academy of Sciences, Beijing 100190, P.R.China
[2]Graduate School of the Chinese Academy of Sciences Beijing 100039, P.R.China

ABSTRACT

We have developed a highly sensitive electric-field sensor with novel comb-shaped microelectrodes. The sensor is based on modulating an incident field with a grounded shutter and measuring the induced charge of sensing electrodes. Owing to the shutter covering the side wall of the sensing electrodes, the fringing fields are no longer a factor that reduces the performance of the sensor. Moreover, in order to improve the efficiency of the charge induction, comb-shaped microelectrodes are introduced. The sensor can measure not only electrostatic field, but also AC field. Tested in ambient air conditions, the minimum detectable field of the sensor is approximately 40V/m with an uncertainty of 1% in DC electric field range 0-50kV/m and 10V/m for a 50Hz AC field. Finally, the use of the sensor to detect ice accretion on high power electric cables is achieved.

KEYWORDS

Electric field sensor, Silicon-on-insulator (SOI), Comb-shaped microelectrodes, Ice accretion detection

INTRODUCTION

Electric-field sensor has wide applications in meteorology, industry, and etc. Recently, the sensor attracts intensive attention in smart grid, e.g. potential application in the measurement of power system voltage, ice accretion detection on high-voltage lines [1], defect detection of insulators [2] and lightning warning.

In recent years, MEMS-based electric-field sensors (MEFS) have given rise to great concern due to their advantages of small size, light weight, easy integration and low power consumption over traditional electric-field sensors. Several MEFS have been developed by different methods, such as electrostatic comb-driven MEFS [3-4] and thermally driven MEFS [5-6]. Most of the reported MEFS used strip sensing electrodes, and had similar induction structure, where the shutter was situated above the sensing electrodes. However, due to the fringing fields at the sidewalls of the shutter, the structures previously reported had low electric field coupling effect for the sensing electrodes, and therefore had lower sensitivity. In addition, in the previous structure, electrodes may be prone to stiction.

This paper presents a novel MEFS based on SOI (silicon-on-insulator) fabrication process. Both the grounded shutter and the differential sensing electrodes are devised in the same structural layer (as shown in Figure 1), therefore the fringing fields is no longer a factor that may reduce the performance of the MEFS. Comb-shaped electrodes are employed to improve the efficiency of charge induction. Consequently, the sensor has a linear response to a wide range of applied electric fields with a high resolution of 40V/m for DC electric field and 10V/m for AC electric field. The experimental results of ice accretion detection for high power electric cables based on the sensor show a potential application in smart grid in the future.

SENSOR DESIGN

Working Principle

The operation principle of the sensor is shown in Figure 1. The grounded shutter travels from side to side within this gap under an applied electric field E_n. When the grounded shutter is in its leftmost position, a larger fraction of the electric field lines terminate on the negative sensing electrode than on the positive sensing electrode, thus the electric field induces more charge on the negative sensing electrode than on the positive one. When the shutter moves to its rightmost position, the situation is reversed-a majority of the electric field lines now terminate on the positive sensing electrode, inducing more charge on it. Consequently, as the grounded shutter oscillates back and forth, it covers the sidewalls of either the positive or negative sensing electrode, then a differential AC current is generated at the sensing electrodes. The output AC current i_{out} of the sensing electrodes is given by:

$$i_{out} = \varepsilon E_n \frac{dA}{dt} \tag{1}$$

where ε is the permittivity of free space, E_n is the component of the electric field normal to the sensing electrodes, A is the effective area of the sensing electrodes.

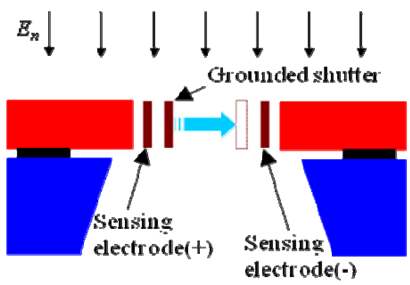

Figure 1: Operating principle of the MEFS.

Structure

A schematic view of the MEFS is shown in Figure 2. The sensor mainly consists of shutter, sensing electrodes, electrostatic comb drives and suspension folded beam. Applying electrostatic comb drives to actuate the shutter allows for better stability and lower power. The shutter is supported by two sets of folded beams that are electrically connected to the grounded plane at two anchor points.

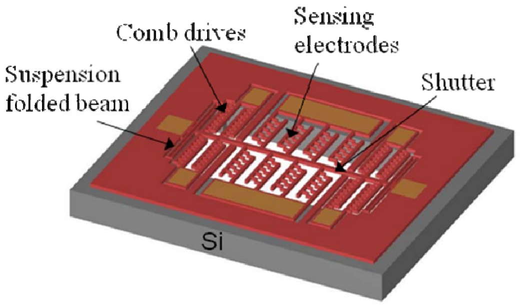

Figure 2: Schematic structure of the MEFS with comb-shaped electrodes.

Differing from the previous structure, both the grounded shutter and the sensing electrodes of the sensor are designed in the same structural layer, this layout of electrodes enhances electric field coupling for the sensing electrodes. Additionally, employing of comb-shaped electrodes can increase the amount of the induced charge on the sensing electrodes and thus improve the sensor sensitivity. The reasons for improving the sensor sensitivity are described in the next section. The MEFS structure is designed to work at the resonant frequency for lower driven voltage and larger oscillating displacement. A fully symmetric structure with differential comb drives and sensing electrodes is used to suppress feed-through into the sensing circuitry and thus improve the signal-to-noise (SNR) of the MEFS.

Electrodes Design

In order to gain higher sensitivity, both optimization and design of electrodes of the sensor are needed. FEM tool was used to simulate and analyze the design with electrostatic solver. First of all, trip electrodes were optimized. The optimization results show that the narrower are the shutter and the sensing electrodes, the more charge variation on the sensing electrodes. Then, we optimize the comb-shaped electrodes structure and get the induced charge variation on comb-shaped sensing electrodes. The simulated results are shown in Table 1.

According to Gauss' law, the amount of charge induced on the sensing electrodes is a function of the strength of the electric field and the effective sensing area. The comb-shaped electrode (as shown in Figure 3) has larger effective sensing area compared with the strip electrode, and thus using comb-shaped electrodes can increase the amount of the induced charge on the sensing electrodes. Finite element simulations illustrated that the charge variation on comb-shaped electrode was 5.2 times than that on the strip electrode under the same conditions of electric field, vibrating displacement and electrodes length. So the comb-shaped electrodes can improve the efficiency of electron charge induction and then improve sensitivity of the MEFS.

Table 1: The charge variation of the unit length of sensing electrode under different electrode geometries.

The type of electrodes		**The amount of charge(C/um)**	
Strip electrode	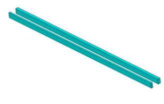	Cover	-12.96E-19
		Expose	-13.38E-19
		Charge variation	**0.42E-19**
Comb-shaped electrode	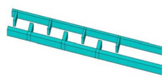	Cover	-8.09E-19
		Expose	-10.27E-19
		Charge variation	**2.18E-19**

FABRICATION AND EXPERIMENTS

Fabrication

The device was prototyped through commercial SOIMUMPS fabrication process, the SEM picture is shown in Figure 3. The SOIMUMPS process is a simple 4-mask level SOI patterning and etching process. The thorough etching of the substrate under the suspended structures significantly reduces the air damping and yields high mechanical quality factors. Another advantage of removing the substrate layer under the suspended structures is that high DC bias voltage can safely be applied to the comb drives, as the effects of electrostatic levitation of the shutter are almost completely eliminated [7]. The SOI MEFS are not prone to stiction compared with the sensor based on polysilicon process and thus more reliable.

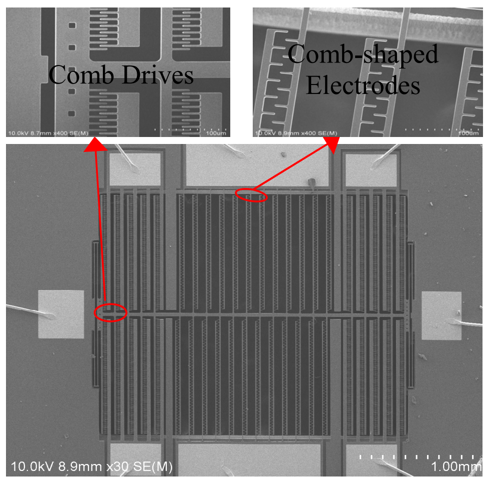

Figure3: SEM photo of the MEFS.

Experiments

Experiments were run in ambient air at room temperature to test the fabricated devices. The sensor was packaged on a DIP 14 metal package. The required uniform electric field was produced by applying a voltage to a large metal plate held 2 cm above the sensor while another large metal plate was electrically connected to the ground. The two large metal plates were positioned just like a parallel plate capacitor.

The sensor was driven by applying 20V DC bias voltage and antisymmetric 1V_{p-p} sinusoidal voltages on both sides of the comb drives. The output signal of the sensing electrodes was processed using a differential amplifier, as shown in Figure 4. Two charge amplifiers converted the output current from the two sets of the sensing electrodes to voltages, which were then subtracted from each other to produce a single voltage proportional to the applied electric field.

With a lock-in amplifier based test system [4], the frequency response was achieved (as shown in Figure 5). The sensor had a quality factor (Q) of approximate 60, and the resonant frequency was 3.042 kHz. In three roundtrip measurements (as shown in Figure 6) at electrostatic field range of 0-50kV/m, the sensor exhibits good performance, with an uncertainty of 1% and minimum detectable field of approximate 40V/m.

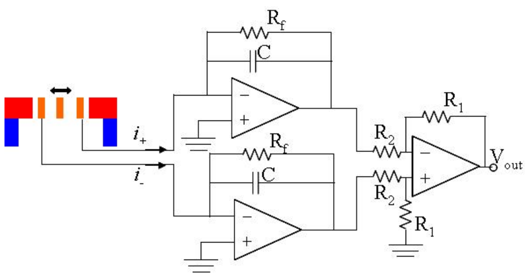

Figure 4: Differential sensing circuitry.

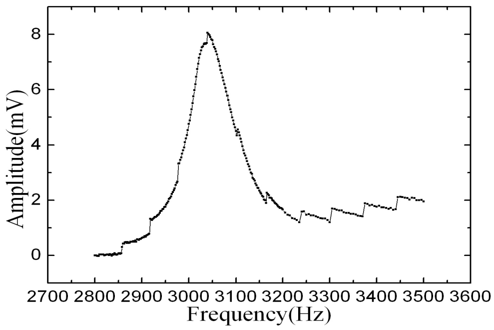

Figure 5: Frequency response of the MEFS. The resonant frequency was 3.042 kHz with a quality factor of 60.

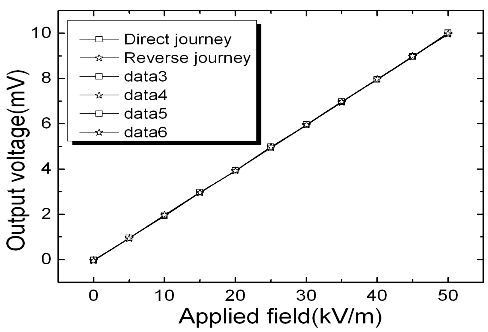

Figure 6: Electrostatic field response of the MEFS. The minimum detectable field was approximate 40V/m with an uncertainty of 1% in three roundtrip measurements.

For smart grid applications, it is required not only measuring electrostatic field but also measuring AC electric field. Differing from DC electric field test system, the test system for AC electric field constructed is based on the way of wireless transferring signal for safety reason. The sinusoidal drive signal of the sensor was produced by singlechip. Both the output signal and the driving signal of the sensor were acquired by wireless data acquisition card. The acquired driving signal was used as reference signal for the output signal of the sensor demodulation. The card sent both the output signal of the sensor and the reference signal to remote PC using the method of wireless communication. The output signal of the sensor received in PC was then filtered and orthogonal demodulated. Accumulator was adopted as the power supply for this test system.

By the test system for AC electric field, our MEFS had been calibrated in a 50Hz AC field and had achieved a high resolution of 10V/m in a measured range of 0-10 kV/m as shown in Figure 7.

According to literature [1], when the ice layer appears on the cable being submitted to high voltage, the electric field around the cable varies significantly with the thickness of the deposited ice. Based on this result, we used the sensor to carry out the research on ice accretion detection for high power electric cables. Primary result was illustrated in Figure 8, which showed that the output of the sensor varied significantly with the thickness of the deposited ice. The experimental results indicated promising potential in future applications.

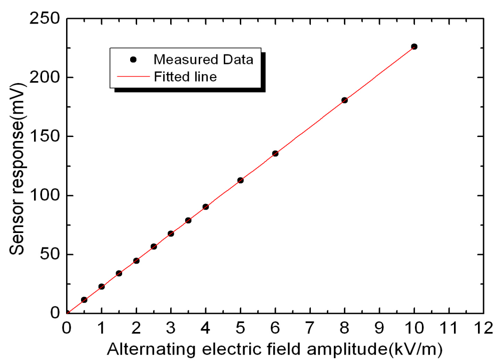

Figure 7: Variation of sensor response with AC field. The minimum detectable field for 50Hz AC field was 10V/m.

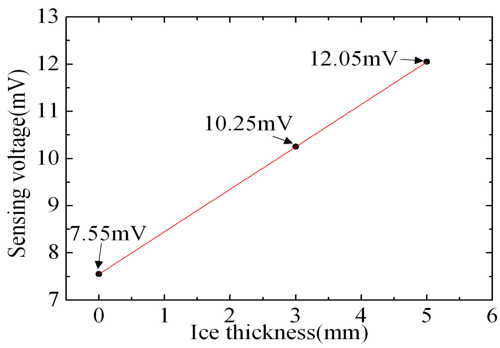

Figure 8: Variation of sensor response with ice thickness.

CONCLUSIONS

The design, simulation, and experiment results for a SOI electric-field sensor were presented. Both the shutter and the differential sensing electrodes were designed in the same plane, by which the sensing electrodes enhanced electric field coupling. The use of comb-shaped electrodes resulted in a significant improvement of the sensor sensitivity. The sensor had a linear response to a wide range of electric fields. The minimum detectable field was 40V/m with an uncertainty of 1% in DC electric field range 0-50kV/m, and 10V/m for AC electric field. For the smart grid applications, we used the sensor to carry out the research on ice accretion detection for high power electric cables. The experimental results showed that the device could detect the thickness of deposited ice on the cable being submitted to high voltage.

ACKNOWLEDGEMENT

This work is financially supported by the National High Technology Research and Development Program of China (863 Program).

REFERENCES

[1] C. barthod, M. passard, J. Bouillot, C. Galez, and M. Farzaneh, "High electric field measurement and ice detection using a safe probe near power installations ", Sensors and Actuators A 113 (2004) pp.140-146.

[2] G. H. Vaillancourt, J. P. Bellerive, M. St-Jean, C. Jean, "New live line tester for porcelain suspension insulators on high-voltage power lines", IEEE Transactions on Power Delivery, Vol. 9 No. 1, January 1994.

[3] P. Riehl, K. Scott, R. Muller, R. Howe, and J. Yasaitis, "Electrostatic charge and field sensors based on micromechanical resonators", J. Microelectromech. Syst., vol.12, no.5, pp. 577-589, Oct. 2003.

[4] C. Peng, X. Chen, Q. Bai, L. Luo, and S. Xia, "A novel high performance micromechanical resonant electrostatic field sensor used in atmospheric electric field detection", in *Proc. 19th IEEE MEMS, Istanbul, Turkey*, Jan. 2006, pp. 698-701.

[5] X. Chen, C. Peng, H. Tao, C. Ye, Q. Bai, S. Chen, and S. Xia, "Thermally driven micro-electrostatic fieldmeter," Sens. Actuators A, Phys., vol. 132, no. 2, pp. 677–682, Nov. 2006.

[6] B.Bahreyni, G.Wijeweera, C.Shafai, A. Rajapakse, "Analysis and Design of a Micromachined Electric-Field Sensor", J. Microelectromech. Syst., vol.17, no.1, pp.31-36, Feb. 2008.

[7] W. C. Tang, M. G. Lim, and R. T. Howe, "Electrostatic Comb Drive Levitation and Control Method", J. microelectromech. Syst., vol. 1, no. 4 pp. 170-178, Dec. 1992.

CONTACT

* Shanhong Xia, tel: +86-10-58887180; shxia@mail.ie.ac.cn